Jpn. J. Appl. Phys. Vol. 42 (2003) pp. L941–L943
Part 2, No. 8A, 1 August 2003

Band Structure of TiO_2-Doped Yttria-Stabilized Zirconia Probed by Soft-X-Ray Spectroscopy

Tohru HIGUCHI*, Kiyoshi KOBAYASHI[1], Shu YAMAGUCHI[2], Akiko FUKUSHIMA[3], Shik SHIN[3,4] and Takeyo TSUKAMOTO

Department of Applied Physics, Tokyo University of Science, 1-3 Kagurazaka, Shinjuku, Tokyo 162-8601, Japan
[1]*National Institute of Advanced Industrial Science and Technology, 1-1-1 Higashi, Tsukuba, Ibaragi 305-8565, Japan*
[2]*Department of Materials Science, University of Tokyo, 7-3-1 Hongo, Bunkyo-ku, Tokyo 113-8656, Japan*
[3]*Institute for Solid State Physics, University of Tokyo, 5-5 Kashiwanoha, Kashiwa, Chiba 277-8581, Japan*
[4]*RIKEN, 1-1-1 Kouto, Mikazuki-cho, Sayo-gun, Hyogo 679-5198, Japan*

(Received May 16, 2003; accepted for publication June 6, 2003)

The electronic structure of TiO_2-doped yttria-stabilized zirconia (YSZ) has been studied by soft-X-ray emission spectroscopy (SXES) and X-ray absorption spectroscopy (XAS). The valence band is mainly composed of the O $2p$ state. The O $1s$ XAS spectrum exhibits the existence of the Ti $3d$ unoccupied state under the Zr $4d$ conduction band. The intensity of the Ti $3d$ unoccupied state increases with increasing TiO_2 concentration. The energy separation between the top of the valence band and the bottom of the Ti $3d$ unoccupied state is in accord with the energy gap, as expected from dc-polarization and total conductivity measurements. [DOI: 10.1143/JJAP.42.L941]

KEYWORDS: yttria-stabilized zirconia (YSZ), TiO_2, X-ray absorption spectroscopy (XAS), soft-X-ray emission spectroscopy (SXES), electronic structure

Mixed-oxide ion conductors have attracted attention due to potential applications such as anode materials in solid-state fuel cells, gas separators for oxygen, and other electrochemical devices for energy conversion systems. Among potential candidates, the most practical mixed-oxide ion conductor is TiO_2-doped yttria-stabilized zirconia (YSZ), which was discovered by Liou and Worrell.[1] The enhancement of the partial conductivity of electrons upon TiO_2 doping into YSZ has been clarified from total conductivity and electronic conductivity measurements by the dc-polarization technique using Hebb-Wagner's asymmetric cell.[2–5] Furthermore, Kobayashi *et al.* have reported the detailed electric properties.[6] The partial conductivity of conduction electrons equilibrated at unit oxygen partial pressure (σ_n°) increases with increasing TiO_2 concentration, and the apparent activation energy of σ_n° decreases upon TiO_2 doping. In contrast, the partial conductivity of holes and the apparent activation energy are almost independent of TiO_2 concentration. These results suggest that the energy gap (E_g) decreases upon TiO_2 doping. Although the decrease of E_g has been observed by electron energy loss spectroscopy (EELS) and ultraviolet photoemission spectroscopy (UPS),[7] the observed electronic structure is strongly affected by the surface structure that is created, due to the degree of correlation and disorder in the surface.

In this study, the electronic structure of TiO_2-doped YSZ ($Zr_{1-x}Y_{0.144}Ti_xO_2$) has been studied by absorption spectroscopy (XAS) and emission spectroscopy (SXES) in the soft-X-ray region. Although photoemission spectroscopy (PES) is a powerful method for studying the electronic structure, PES is surface sensitive, because the mean free path of an electron is very short compared with that of light. XAS and SXES techniques can be used to investigate the electronic structure of the bulk state since the mean free path of a soft-X-ray is very long compared with that of an electron. XAS is related directly to the unoccupied density-of-state (DOS).[8,9] Its optical process is a rather local process, because of the localized core state. It is governed by the dipole selection rules so that XAS gives a spectrum corresponding to the site- and symmetry-selected DOS. SXES is related directly to the occupied DOS.[10,11] The partial DOS (PDOS) localized at the atom can be obtained from SXES spectra, because SXES involves a clear selection rule regarding the angular momentum due to dipole selection.

The $Zr_{1-x}Y_{0.144}Ti_xO_2$ samples were sintered ceramics prepared by a conventional solid-state reaction method. The starting materials were YSZ powder with 99.9% purity supplied by Tosoh Co Ltd. and TiO_2 powder with 99.99% purity supplied by Rare Metallic Co. Ltd. The sample rods, prepared by isotopic pressing of well-mixed powder, were calcined at 1673 K for 10 h in air. Then, the samples were crushed into powder and mechanically pressed into disks. Finally, the disks were sintered at 1873 K for 10 h in air. The TiO_2 concentrations were $x = 0.019$, $x = 0.046$ and $x = 0.093$. The samples were confirmed as being of a single phase by powder X-ray diffraction analysis.

XAS and SXES spectra were measured using a soft-X-ray spectrometer installed at the undulator beamline BL-19B (in Photon Factory) at the High Energy Accelerator Organization. Synchrotron radiation was monochromatized using a varied-line spacing plane grating whose average groove density was 1000 lines/mm. The spectra were measured in a polarized configuration. The energy resolution of XAS was about 0.1 eV at $h\nu = 450$ eV. The energy resolution of SXES was about 0.5 eV at $h\nu = 500$ eV. The bottom axis was calibrated by measuring the $4f$ core level of Au film.

Figure 1(a) shows the O $1s$ XAS spectrum of $Zr_{0.837}Y_{0.144}Ti_{0.019}O_2$. From the dipole selection rule, it is understood that the O $1s$ XAS spectra of the $4d$ transition metal oxide correspond to the transitions from O $1s$ to O $2p$ characters hybridized into the unoccupied metal $4d$ states. Two peaks at around ~533.5 eV and 537.0 eV correspond to the t_{2g}- and e_g-subbands, respectively. Four vertical bars, which are labeled from 1 to 4, indicate the excitation energies selected for the resonant SXES measurements.

Figure 1(b) shows the O $1s$ resonant SXES spectra of $Zr_{0.837}Y_{0.144}Ti_{0.019}O_2$. The O $1s$ emission reflects the O $2p$ PDOS in the valence band region. The arrow indicates the elastic scattering peak, which corresponds to the excitation photon energy. Two features, A and B, are observed at ~525.0 eV and 523.6 eV, respectively. Although the intensity of feature B does not depend on the photon excitation,

*E-mail address: higuchi@rs.kagu.tus.ac.jp

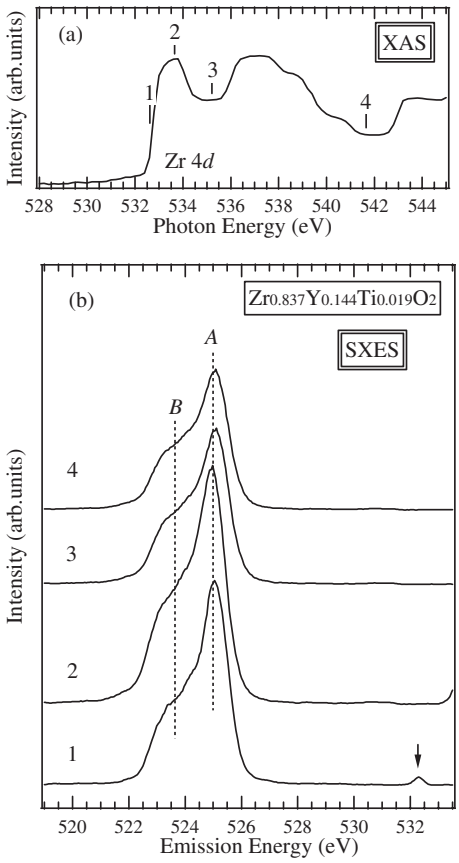

Fig. 1. (a) O 1*s* XAS spectrum of $Zr_{0.837}Y_{0.144}Ti_{0.019}O_2$. The numbers indicate the photon energies at which the resonant SXES spectra were measured. (b) O 1*s* SXES spectra of $Zr_{0.837}Y_{0.144}Ti_{0.019}O_2$ excited at various photon energies indicated in Fig. 1(a). Arrow shows the peak position of the elastic scattering. *A* and *B* indicate the O 2*p* fluorescence components.

that of feature *A* is enhanced at the excitation energy corresponding to the t_{2g} absorption peak, indicating the O 1*s* $\rightarrow$ 2*p* resonance effect. However, the O 1*s* resonant SXES spectra are not found to the exist by soft-X-ray Raman scattering, which is often useful for observing resonant SXES spectra excited at transition metal sites. Therefore, the O 1*s* resonant SXES spectra of $Zr_{0.837}Y_{0.144}Ti_{0.019}O_2$ reflect the O 2*p* fluorescence component in the valence band region. On the other hand, the spectral lineshape and peak position resemble with those of ZrO_2[12,13] and In-doped $CaZrO_3$,[14,15] which have the same electronic configuration as YSZ. It is reported that the Zr 4*d* contribution is more significant on the higher binding energy side of the valence band, where the bonding O 2*p* states have a larger admixture of Zr 4*d* states. For In-doped $CaZrO_3$,[14,15] *A* and *B* peaks corresponding to those in the SXES spectrum of $Zr_{0.837}Y_{0.144}Ti_{0.019}O_2$ are estimated to represent the non-bonding state and the bonding state that is well mixed with the Zr 4*d* state, respectively. Such a situation is also expected for $Zr_{1-x}Y_{0.144}Ti_xO_2$.

Figure 2 shows the O 1*s* SXES spectra as a function of TiO_2 concentration in $Zr_{1-x}Y_{0.144}Ti_xO_2$. The intensities of the SXES spectra are normalized by the beam current and measurement time. With this normalization, it is evident that the intensity of elastic scattering in the sample with $x = 0.019$ is in good agreement with those in samples with $x = 0.046$ and $x = 0.093$. The dashed line at ~526.0 eV indicates the position of the top of the valence band. Comparing each SXES spectrum, one can see that the bandwidth and peak positions do not depend on the TiO_2 concentration. This behavior is in accordance with the results of UPS.[7]

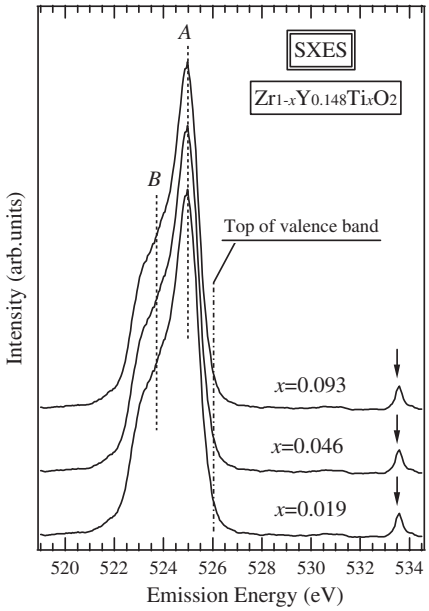

Fig. 2. O 1*s* SXES spectra as a function of TiO_2 concentration in $Zr_{1-x}Y_{0.144}Ti_xO_2$. The SXES spectrum when $x = 0.019$ is spectrum 2 in Fig. 1(b). Arrows show the peak positions of elastic scattering.

Figure 3 shows the O 1*s* XAS spectra as a function of TiO_2 concentration in $Zr_{1-x}Y_{0.144}Ti_xO_2$. The O 1*s* XAS spectra are normalized by the e_g-subband of the Zr 4*d* state. The dashed line at ~526.0 eV shows the top of the valence band, which is estimated from the O 1*s* SXES spectra in Fig. 2. The feature around at 533.4 eV corresponds mainly to the Zr 4*d* state hybridized with the O 2*p* state. The spectral intensity depends on TiO_2 concentration. The change is

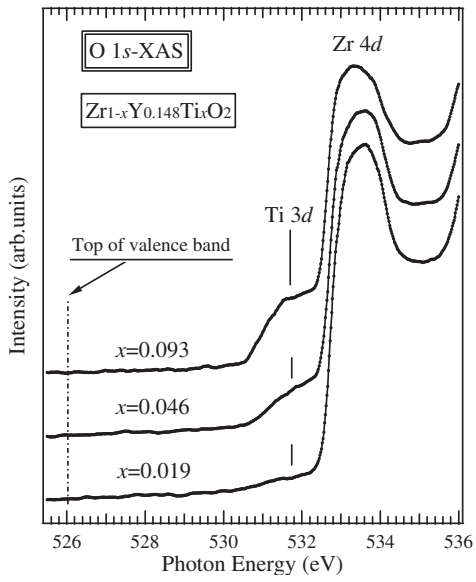

Fig. 3. O 1*s* XAS spectra as a function of TiO_2 concentration in $Zr_{1-x}Y_{0.144}Ti_xO_2$. The XAS spectrum when $x = 0.019$ is the spectrum in Fig. 1(a). Dashed line shows the top of the valence band.

believed to originate in the difference in the hybridization effects between Zr 4*d* and O 2*p* states with TiO_2 concentration.

It is striking that a prominent feature at 531.6 eV is observed under the bottom of the Zr 4*d* conduction band. The intensity increases with increasing TiO_2 concentration. Therefore, this feature is assigned to the unoccupied Ti 3*d* state created by TiO_2 doping. The energy separation between the top of the O 2*p* valence band and the bottom of the Ti 3*d* unoccupied state may give the energy gap (E_g) of $Zr_{1-x}Y_{0.144}Ti_xO_2$. The estimated E_g is about 5.3 eV when $x = 0.019$ and about 4.7 eV when $x = 0.046$ and $x = 0.093$. These values are in good agreement with the E_g calculated from the dc-polarization and total conductivity measurements.[6] Furthermore, the energy separation (ΔE) between the Zr 4*d* state and the Ti 3*d* state in $Zr_{1-x}Y_{0.144}Ti_xO_2$ measured by the coloration method has been suggested to be 1.8 eV.[16] Because the E_g value when $x = 0$ is about 6.4 eV, the ΔE value is found to be close to the difference between the E_g value when $x = 0$ and that when $x = 0.046$ or $x = 0.093$. The ΔE value is also in accord with the O 1*s* XAS spectra in Fig. 3.

In conclusion, we have studied the electronic structure of $Zr_{1-x}Y_{0.144}Ti_xO_2$ using XAS and SXES techniques. The valence band is mainly composed of the O 2*p* state, though the contribution of the Zr 4*d* state also exists. The O 1*s* XAS spectra exhibit the unoccupied Ti 3*d* state under the bottom of the Zr 4*d* conduction band. The energy separation between the Ti 3*d* state and the Zr 4*d* state is about 1.8 eV. E_g, which corresponds to the energy separation between the top of the O 2*p* valence band and the bottom of the Zr 4*d* conduction band, is about 5.3 eV when $x = 0.019$ and about 4.6 eV when $x = 0.046$ and $x = 0.093$. These values are in good agreement with the results calculated from the dc-polarization and total conductivity measurements.

This work was partially supported by the Foundation for Materials Science and Technology of Japan (MST Foundation), and the Grant-In-Aid for Scientific Research from the Ministry of Education, Cultures, Sports, Science and Technology.

1) S. S. Liou and W. L. Worrell: Appl. Phys. A **49** (1989) 25.
2) H. Naito and H. Arashi: Solid State Ionics **53–56** (1992) 436.
3) K. Kobayashi, K. Kato, T. Kawashima, S. Yamaguchi and Y. Iguchi: J. Ceram. Soc. Jpn. **106** (1998) 1073.
4) K. Kobayashi, Y. Kai, S. Yamaguchi, N. Fukatsu, T. Kawashima and Y. Iguchi: Solid State Ionics **93** (1997) 193.
5) K. Kobayashi, Y. Kai, S. Yamaguchi, T. Kawashima and Y. Iguchi: J. Ceram. **4** (1998) 114.
6) K. Kobayashi, S. Yamaguchi, T. Higuchi, S. Shin and Y. Iguchi: Solid State Ionics **135** (2000) 643.
7) U. Vohrer, H.-D. Wiemhöfer, W. Göpel, B. A. van Hassel and A. J. Burggraaf: Solid State Ionics **59** (1993) 141.
8) T. Higuchi, T. Tsukamoto, K. Kobayashi, Y. Ishiwata, M. Fujisawa, T. Yokoya, S. Yamaguchi and S. Shin: Phys. Rev. B **61** (2000) 12860.
9) T. Higuchi, T. Tsukamoto, K. Kobayashi, S. Yamaguchi, Y. Ishiwata, N. Sata, K. Hiramoto, M. Ishigame and S. Shin: Phys. Rev. B **65** (2002) 33201.
10) T. Higuchi, T. Tsukamoto, M. Watanabe, M. M. Grush, T. A. Callcott, R. C. Perera, D. L. Ederer, Y. Tokura, Y. Harada, Y. Tezuka and S. Shin: Phys. Rev. B **60** (1999) 7711.
11) T. Higuchi, M. Tanaka, K. Kudoh, T. Takeuchi, Y. Harada, S. Shin and T. Tsukamoto: Jpn. J. Appl. Phys. **40** (2001) 5803.
12) C. Morant, A. Fernandez, A. R. Gonzalez-Elipe, L. Soriano, A. Stampfl, A. M. Bradshaw and I. M. Sanz: Phys. Rev. B **52** (1995) 11711.
13) H. J. F. Jansen: Phys. Rev. B **43** (1991) 7267.
14) T. Higuchi, S. Yamaguchi, K. Kobayashi, T. Takeuchi, S. Shin and T. Tsukamoto: Jpn. J. Appl. Phys. **41** (2002) L938.
15) T. Higuchi, T. Tsukamoto, Y. Tezuka, K. Kobayashi, S. Yamaguchi and S. Shin: Jpn. J. Appl. Phys. **39** (2002) L133.
16) N. Nicoloso, R. I. Merino, H. Yugami and J. Maier: *Proc. 1st Int. Symp. Ceram. Membranes* (1997) p. 106.